# Supporting Information for Surface Functionalized Atomic Layer Deposition of Bismuth Vanadate for Phase Pure Scheelite

Benjamin Lamm, Amrita Sarkar, and Morgan Stefik*
Department of Chemistry and Biochemistry, University of South Carolina, Columbia, SC 29208.
*morgan@stefikgroup.com

**Estimation of Host-Guest Architecture Needed for Efficient Light Harvesting**

Host-guest architectures allow the decoupling of optical absorption from carrier transport. Here we consider the characteristics needed for a host-guest architecture based upon 30 nm SF-ALD $BiVO_4$ films. Within the 2.4 eV bandgap of $BiVO_4$,[1–3] the AM 1.5 spectrum has the most photon flux near the band-edge at 510 nm. Considering a target of 90% light harvesting efficiency at the 510 nm band edge, the corresponding optical thickness may be calculated using equation S1:

$$A = \alpha l \quad \text{(S1)}$$

where A, α, and *l* are the absorbance, attenuation coefficient, and optical thickness of the film. The attenuation of a 30 nm film may thus be used to calculate the optical thickness needed for 90% light harvesting via the attenuation coefficient. Here the absorbance was calculated from the measured absorptance value using equation S2:

$$A = -log(1 - \frac{A_{\%}}{100}) \quad \text{(S2)}$$

where $A_{\%}$ is the absorptance as a percentage. The attenuation coefficient of the 30 nm MeOH-SF-ALD film was thus calculated to be 0.001433 $nm^{-1}$(at λ=510 nm). This attenuation coefficient was thus used to calculate that 90% absorptance would occur with an optical thickness of 697 nm. This value provides considerable insight into the design of host-guest architectures with efficient light harvesting. For example, assuming all layers are normal to the incident light, this optical thickness corresponds to a roughness factor of (697 nm)/(30 nm)=23.2. In other words, 23.2 such 30 nm layers would be needed to reach the described light harvesting target.

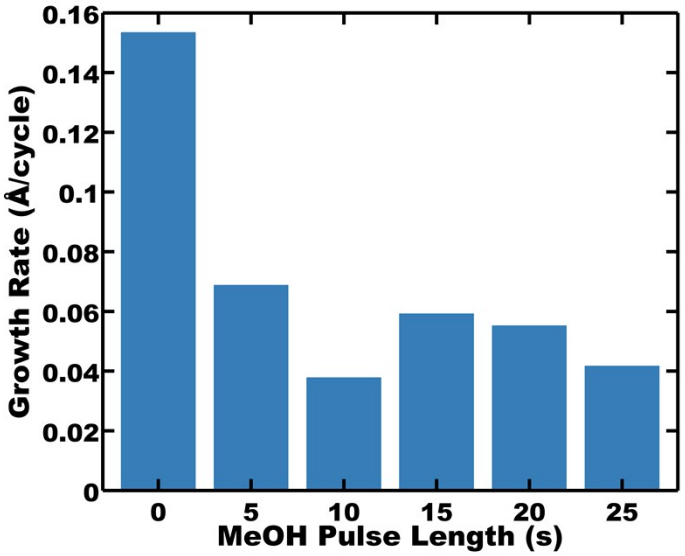


Figure S1. The MeOH pulse length was optimized to saturate the inhibition of $V_2O_5$ growth using a pulse sequence of $[MeOH\text{-}VTIP\text{-}W]_x$.

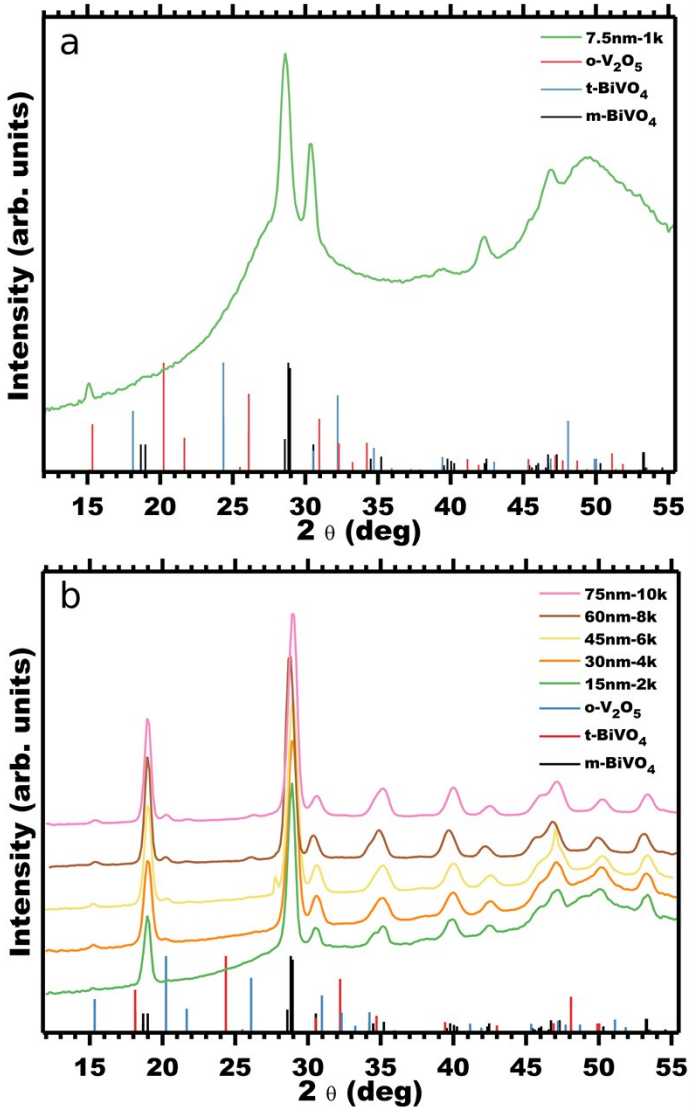


Figure S2. GIWAXS of calcined MeOH-BVO films of 7.5 (a) and 15-75 nm (b) thickness. Sample descriptions in Table 4 of the text.

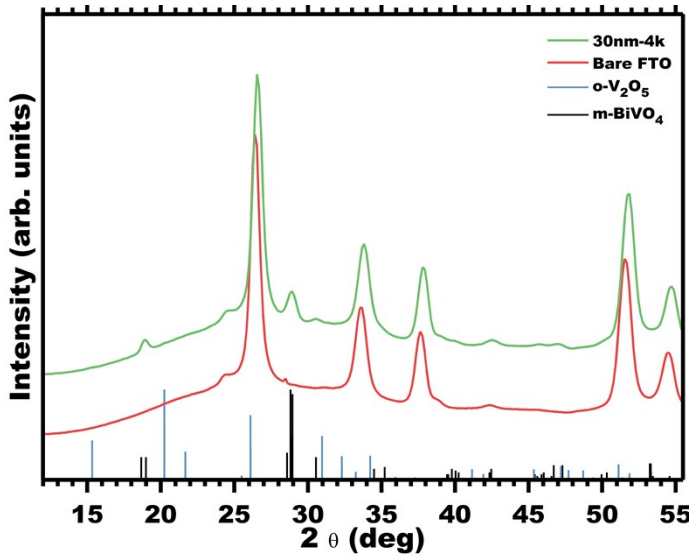


Figure S3. GI-WAXS of bare FTO and FTO/$BiVO_4$ (30 nm, calcined MeOH-BVO where x=4,000 cycles).

Table S1. Comparison of mean front-side photocurrent at 0.6 V vs RHE ($J_{J\text{-}V}$) to photocurrent calculated from IPCE ($J_{IPCE}$). Data is from calcined SF-BVO films. Samples are the same as those described in Table 4 of the text. $J_{IPCE}$ was determined by multiplying IPCE (%) by the AM 1.5 spectrum (mA/cm²/nm) before integrating over wavelength (nm).

| Sample Name | $J_{J\text{-}V}$ (mA/cm²) | $J_{IPCE}$ (mA/cm²) | Percent Difference |
|---|---|---|---|
| 7.5nm-1k | 0.010±0.002 | 0.003±0.001 | 63.9 |
| 15nm-2k | 0.075±0.005 | 0.026±0.005 | 64.6 |
| 22.5nm-3k | 0.11±0.01 | 0.043±0.007 | 62.4 |
| 30nm-4k | 0.35±0.01 | 0.20±0.02 | 44.4 |
| 45nm-6k | 0.31±0.02 | 0.18±0.03 | 42.2 |
| 60nm-8k | 0.46±0.02 | 0.33±0.03 | 29.4 |
| 75nm-10k | 0.57±0.03 | 0.66±0.03 | 15.2 |

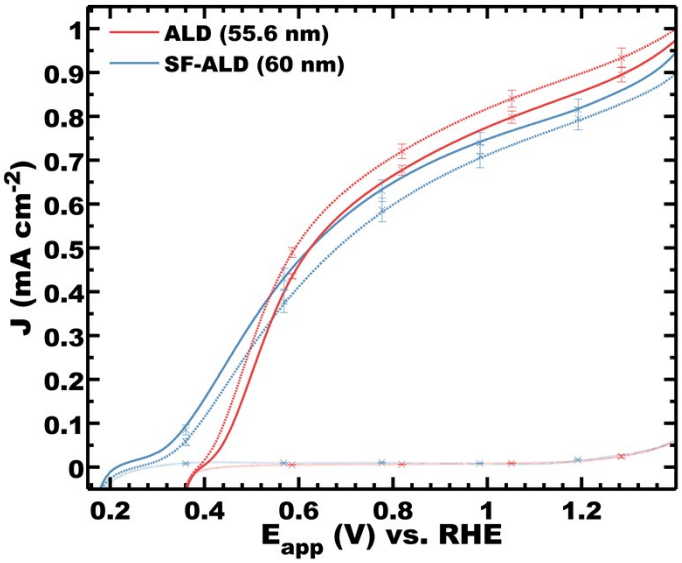


Figure S4. The photocurrent performance of bismuth vanadate films prepared by conventional ALD and SF-ALD were compared under simulated AM 1.5 illumination. The conventional ALD procedure is identical to the SF-ALD procedure sans alcohol surface functionalization. The conventional ALD samples were 55.6 nm thick and were calcined at 450 °C for 1 hr and etched in 1 M NaOH to remove excess $V_2O_5$. The comparable SF-ALD samples were denoted at **60nm-8k** in the text.

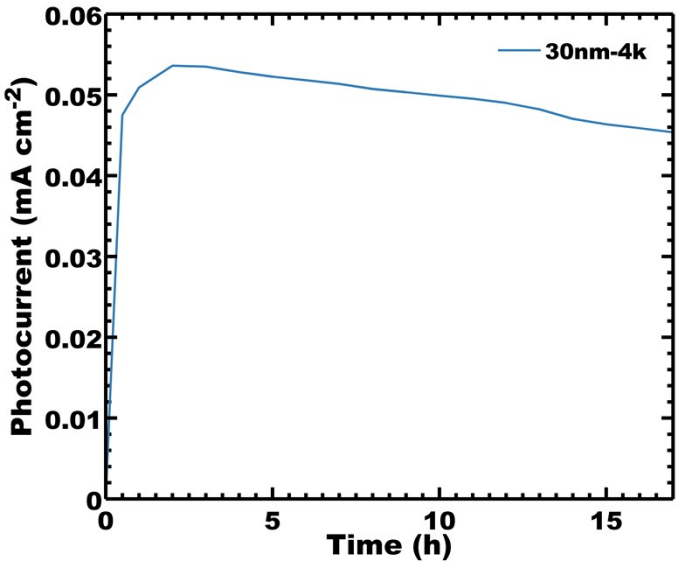


Figure S5. Chronoamperometry of SF-ALD film 30nm-4k over 17hrs of continuous simulated AM 1.5 illumination at an applied potential of 0.6 V vs RHE. The electrolyte was 1.0 M potassium borate with a pH of 9.36 with 0.2 M $Na_2SO_3$ as hole scavenger.

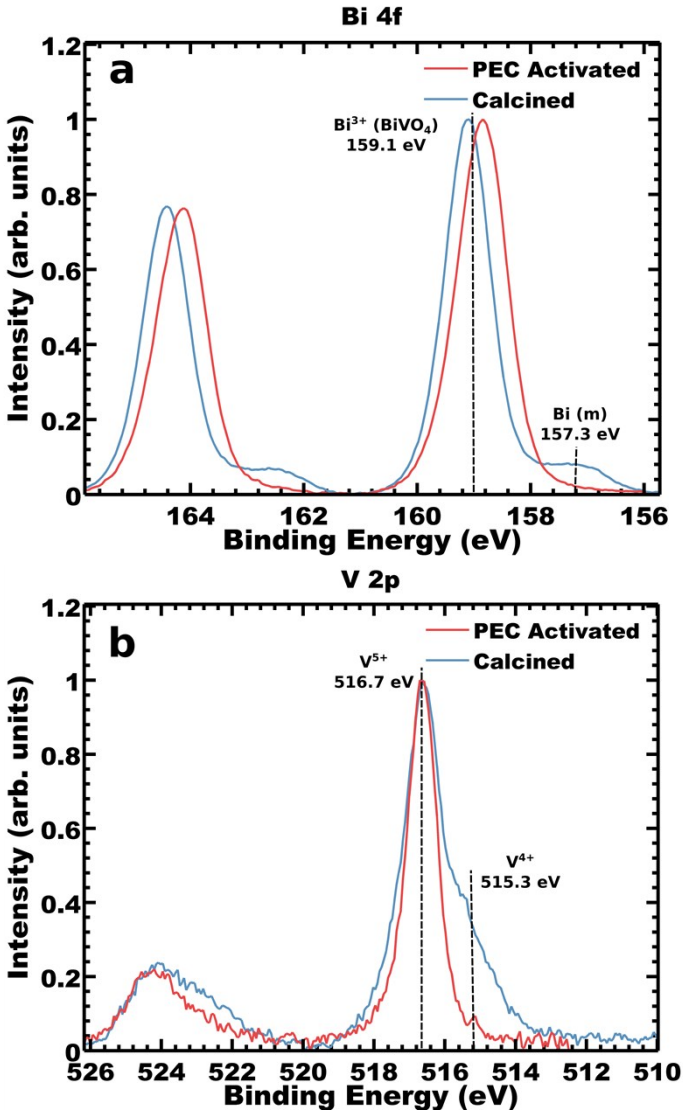


Figure S6. XPS of calcined and PEC activated 30nm-4k films, showing regions for (a) Bi 4f and (b) V 2p.

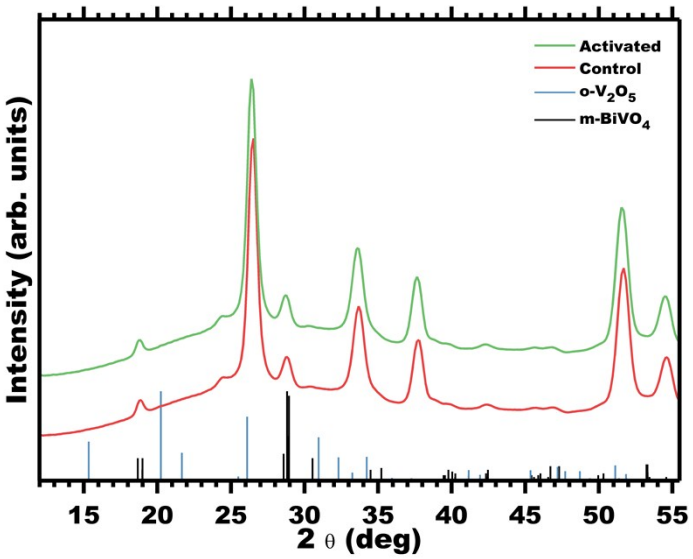


Figure S7. GI-WAXS measurements on calcined 30 nm MeOH-BVO films without and with the photoelectrochemical activation. **Control** and **Activated** samples are the same as those described in Table 6 of the main text.

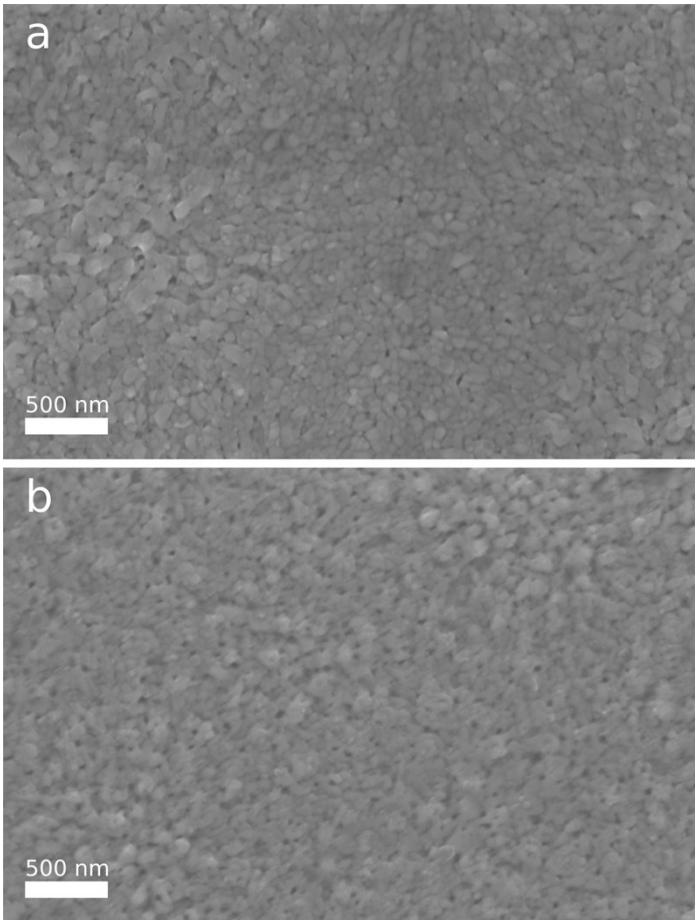


Figure S8. Comparison of surface structure (a) before and (b) after photoelectrochemical activation. Images were acquired on calcined 30 nm MeOH-BVO films deposited on FTO.

Table S2. All parameters used in the MeOH-SF-ALD deposition.

| Step | Label | Device Index | Device Name | Action | Value | Branch |
|---|---|---|---|---|---|---|
| 1 | | 28 | Pump | | 0 | |
| 2 | | 9 | EXPO_Heater | Set_to_On | 0 | |
| 3 | | 8 | MFC_Flow | Set_to_Value | 200 | |
| 4 | | 1 | VTIP Heater | Set_to_Value | 45 | |
| 5 | | 2 | BiPh3 Heater | Set_to_Value | 130 | |
| 6 | | 4 | Metal Precursor Manifold | Set_to_Value | 130 | |
| 7 | | 5 | Oxidant Manifold | Set_to_Value | 130 | |
| 8 | | 7 | Chamber_Door_Heat | Set_to_Value | 130 | |
| 9 | | 6 | Chamber_Heat | Set_to_Value | 130 | |
| 10 | | 6 | Chamber_Heat | Wait_Until_Set_Point_+/- | 1 | |
| 11 | | 22 | Delay_(Sec.) | | 7200 | |
| 12 | **DepoLoop** | 22 | Delay_(Sec.) | | 0.1 | |
| 13 | **VLoop** | 8 | MFC_Flow | Set_to_Value | 40 | |
| 14 | | 8 | MFC_Flow | Wait_Until_< | 45 | |
| 15 | | 10 | EXPO_Actuator | Set_to_Closed | 0 | |
| 16 | | 22 | Delay_(Sec.) | | 0.2 | |
| 17 | MeOH | 18 | ALD_7_Actuator | Pulse_(mSec.) | 25 | |
| 18 | | 22 | Delay_(Sec.) | | 1 | |
| 19 | | 10 | EXPO_Actuator | Set_to_Open | 0 | |
| 20 | | 8 | MFC_Flow | Set_to_Value | 200 | |
| 21 | | 22 | Delay_(Sec.) | | 10 | |
| 22 | | 8 | MFC_Flow | Set_to_Value | 5 | |
| 23 | | 8 | MFC_Flow | Wait_Until_< | 6 | |
| 24 | | 22 | Delay_(Sec.) | | 7 | |
| 25 | | 10 | EXPO_Actuator | Set_to_Closed | 0 | |
| 26 | | 22 | Delay_(Sec.) | | 0.2 | |
| 27 | VTIP | 13 | ALD_2_Actuator | Pulse_(mSec.) | 2000 | |
| 28 | | 22 | Delay_(Sec.) | | 1 | |
| 29 | | 10 | EXPO_Actuator | Set_to_Open | 0 | |
| 30 | | 8 | MFC_Flow | Set_to_Value | 200 | |
| 31 | | 22 | Delay_(Sec.) | | 10 | |
| 32 | | 8 | MFC_Flow | Set_to_Value | 40 | |
| 33 | | 8 | MFC_Flow | Wait_Until_< | 45 | |
| 34 | | 10 | EXPO_Actuator | Set_to_Closed | 0 | |
| 35 | | 22 | Delay_(Sec.) | | 0.2 | |
| 36 | water | 16 | ALD_5_Actuator | Pulse_(mSec.) | 25 | |
| 37 | | 22 | Delay_(Sec.) | | 1 | |
| 38 | | 10 | EXPO_Actuator | Set_to_Open | 0 | |
| 39 | | 8 | MFC_Flow | Set_to_Value | 200 | |
| 40 | | 22 | Delay_(Sec.) | | 10 | |
| 41 | | 24 | Loop_n_Times | Number | 1 | **VLoop** |

| | | | | | | |
|---|---|---|---|---|---|---|
| 42 | **BiLoop** | 8 | MFC_Flow | Set_to_Value | 40 | |
| 43 | | 8 | MFC_Flow | Wait_Until_< | 45 | |
| 44 | | 11 | N2_Inject | | 0 | |
| 45 | | 10 | EXPO_Actuator | Set_to_Closed | 0 | |
| 46 | | 22 | Delay_(Sec.) | | 0.2 | |
| 47 | BiPH3 | 14 | ALD_3_Actuator | Pulse_(mSec.) | 2000 | |
| 48 | | 22 | Delay_(Sec.) | | 1 | |
| 49 | | 10 | EXPO_Actuator | Set_to_Open | 0 | |
| 50 | | 8 | MFC_Flow | Set_to_Value | 200 | |
| 51 | | 22 | Delay_(Sec.) | | 10 | |
| 52 | | 8 | MFC_Flow | Set_to_Value | 40 | |
| 53 | | 8 | MFC_Flow | Wait_Until_< | 45 | |
| 54 | | 10 | EXPO_Actuator | Set_to_Closed | 0 | |
| 55 | | 22 | Delay_(Sec.) | | 0.2 | |
| 56 | water | 16 | ALD_5_Actuator | Pulse_(mSec.) | 25 | |
| 57 | | 22 | Delay_(Sec.) | | 1 | |
| 58 | | 10 | EXPO_Actuator | Set_to_Open | 0 | |
| 59 | | 8 | MFC_Flow | Set_to_Value | 200 | |
| 60 | | 22 | Delay_(Sec.) | | 10 | |
| 61 | | 24 | Loop_n_Times | Number | 1 | **BiLoop** |
| 62 | | 24 | Loop_n_Times | Number | 3000 | **DepoLoop** |
| 63 | | 22 | Delay_(Sec.) | | 3600 | |
| 64 | | 8 | MFC_Flow | Set_to_Value | 5 | |

**References**


(1) Kudo, A.; Omori, K.; Kato, H. A Novel Aqueous Process for Preparation of Crystal Form-Controlled and Highly Crystalline BiVO 4 Powder from Layered Vanadates at Room Temperature and Its Photocatalytic and Photophysical Properties. *J. Am. Chem. Soc.* **1999**, *121*, 11459–11467.

(2) Kim, T. W.; Choi, K.-S. Nanoporous BiVO4 Photoanodes with Dual-Layer Oxygen Evolution Catalysts for Solar Water Splitting. *Science (80-. ).* **2014**, *343* (6174), 990–994.

(3) Park, Y.; McDonald, K. J.; Choi, K.-S. Progress in Bismuth Vanadate Photoanodes for Use in Solar Water Oxidation. *Chem. Soc. Rev.* **2013**, *42* (6), 2321–2337.